Journal of Polymers and the Environment (2023) 31:541–551
https://doi.org/10.1007/s10924-022-02633-9

ORIGINAL PAPER

Valorization of Waste Wood Flour and Rice Husk in Poly(Lactic Acid)-Based Hybrid Biocomposites

László Lendvai[1,2] · Maria Omastova[2] · Amar Patnaik[3] · Gábor Dogossy[1] · Tej Singh[4]

Accepted: 10 October 2022 / Published online: 2 November 2022

Abstract

This study explores the possibility of developing a new class of hybrid particulate-filled biocomposites using wood flour and rice husk wastes as environmentally friendly additives to poly(lactic acid) (PLA) as matrix material. Samples were prepared with fillers of different concentrations (0, 2.5, 5, 7.5 and 10 wt %), while the ratio of wood flour and rice husk was fixed at 1:1 in all cases. The preparation of biocomposites was performed through extrusion using a twin-screw extruder. Subsequently, they were formed into specimens by injection molding. Mechanical, thermal, thermomechanical, and morphological properties were examined. The addition of natural waste particles resulted in a remarkable improvement both in tensile and flexural modulus; however at a cost of impact strength and tensile strength. Meanwhile, flexural stress at conventional strain values were barely affected by the presence of wood flour and rice husk. The SEM images confirmed that there is a limited interfacial adhesion between the components, which supports the results obtained during mechanical tests. Both the differential scanning calorimetry (DSC) and the dynamic mechanical analysis indicated that the glass transition temperature of PLA was not affected by the incorporation of filler particles; however, the crystalline structure was gradually altered with increasing filler loading according to the DSC. Additionally, the particles were observed acting as nucleating agents, thereby increasing the overall crystallinity of PLA.

Keywords Poly(lactic acid) · Wood flour · Rice husk · Biocomposite · Mechanical properties · Structure-property relationships

Introduction

Recently, growing environmental concerns have made it imperative to replace as much petrochemical plastics as possible with sustainable biopolymers [1]. The research and development of such biobased and compostable materials is also greatly spurred by growing oil-shortages and energy demand. Among the polymers obtained from renewable resources, poly(lactic acid) (PLA) is one of the most versatile materials.

PLA is a thermoplastic polyester produced by the polymerization of lactic acid monomer. Lactic acid is generally derived from starch-rich agricultural feedstocks (corn, wheat, sugarcanes, etc.) through fermentation [2]. Considering its properties, PLA is a promising substitute for conventional petrol-based plastics for various applications, including packaging, biomedical equipment, and automotive components as well [1, 3]. Its excellent strength and stiffness and good processability make PLA comparable to other conventional polymers, like polystyrene or polyethylene-terephthalate. Despite all these qualities, PLA has some major drawbacks that hinder its spread, such as brittleness, low thermal stability, and high production costs. Unless its price can be reduced from its current level (~4–5 €/kg), its large-scale market penetration is not expected [4]; consequently, the development of PLA-based polymer blends [5–7] and composites [8–10] with low-cost secondary components have drawn a large body of scientific interest over

✉ László Lendvai
lendvai.laszlo@sze.hu

1 Department of Materials Science and Engineering, Széchenyi István University, Egyetem tér 1, Győr H-9026, Hungary

2 Polymer Institute, Slovak Academy of Sciences, Dubravska cesta, 9, 845 41 Bratislava, Slovakia

3 Department of Mechanical Engineering, Malaviya National Institute of Technology, Jaipur 302017, India

4 Savaria Institute of Technology, Eötvös Loránd University, Károlyi Gáspár tér 4, Szombathely H-9700, Hungary

the last several years. Besides, numerous studies have been devoted to the preparation of PLA-based composites filled with innovative nanoparticles to improve the mechanical and thermal properties of this biopolymer [11, 12]. In order to preserve its "green" characteristics, PLA is mostly paired with polymers and additives that are also derived from natural sources themselves.

The utilization of low-cost filler materials for the sake of price reduction is commonly applied in the plastic industry. Generally, residues originating from industrial and agricultural processes are used for this purpose [13]. Incorporating these by-products into polymeric materials does not only cut back the production costs, but also promotes the sustainable development through finding a suitable function for these waste materials that would be otherwise dumped or burned. Such by-products, including the various forest industry- and agricultural residues, are abundantly available natural materials. In many countries, these residues are being disposed of through open burning, which is responsible for serious deterioration of air quality, thereby also affecting public health. Rice husk (RH) is a waste that is separated from rice grains throughout the milling process. According to the literature, for every ton of rice produced, 0.23 tons of RH is also generated [14]. Considering the fact that average worldwide rice production was approximately 500 million metric tons annually between 2017 and 2021, the RH formed per year exceeds 100 million metric tons [15]. This immense amount of waste biomass presents a major disposal issue, especially in countries with the most production (China, India, Indonesia). RH contains cellulose (~35%) hemicellulose (~35%), lignin (~20%), and ash (10%) [16]. Since the nutrient value of RH is rather poor and its composting time is also relatively long due to its high lignin content, the rice husk is often used as a source of cheap energy through combustion, which greatly contributes to environmental pollution [14, 17]. As a consequence, a large body of work has been published on the topic of reusing RH in a sustainable way, including its incorporation into polymer matrices to act as reinforcement [13, 18–20].

Mu et al. [21] fabricated high density polyethylene (HDPE)-based composites with the incorporation of various agricultural residues, namely rice straw, RH, wheat straw, sugarcane cotton stalk, bagasse and bamboo. Even though the rice husk proved to be the least effective reinforcement particle out of the listed ones, it still improved both the tensile (~18 MPa => ~21 MPa) and flexural strength (~21 MPa => ~39 MPa) of HDPE. Similarly, the tensile (~1.1 GPa => ~3.5 GPa) and flexural (~0.8 GPa => ~3.3 GPa) moduli were also greatly enhanced; however, at a cost of impact resistance (~31 kJ/m^2 => ~7.5 kJ/m^2). Farhan Zahar and Siddiqui [22] incorporated RH of three different sizes (250–355 µm, 355–500 µm, 500,710 µm) at three different loading (5%, 10%, 15%) into polystyrene matrix. They reported a maximum tensile strength at 5% concentration for RH with a size of 355–500 µm, which was attributed to the best dispersion of the filler particles for this specific composition.

Other than RH, there is a considerable number of other low-cost natural fillers used in polymeric composites. Among the various bio-fillers, wood is the most widespread. It has been effectively used as an additive in numerous polymer matrices for decades now. While previously it has only been embedded into petrochemical commodity plastics; lately, there is a progressively growing number of studies dealing with its incorporation into bio-based and/or biodegradable plastics, like PLA. Borysiuk et al. [23] introduced bark wood filler into PLA-based composites at different concentrations and different sizes (10–35 mesh, 35 mesh+). It was found that with increasing bark content the modulus of elasticity and modulus of rupture of the fabricated samples deteriorated. Regarding the particles' size, the larger ones were preferable considering the mechanical and physical properties. Andrzejewski et al. [24] fabricated composites filled with cork/wood in the amount of 0–30 wt%. PLA and polypropylene (PP) were used as matrix materials. Regardless of the type of additive, the tensile strength and the elongation at break of both PLA and PP decreased with increasing filler content. The authors also concluded that wood was superior in comparison with cork in terms of strength and stiffness, while cork was an effective agent to improve the dimension stability of the polymers in the presence of moisture.

The various agricultural- and forest industry wastes tend to exhibit greatly varying physical and mechanical properties. This fact has recently driven some researchers to fabricate composites by incorporating multiple types of biofillers at the same time, thereby creating hybrid composites. The hybrid approach makes it possible to exploit the potential of both additives, and in some specific cases a synergistic effect might also occur. Anggono et al. [25] developed PLA-based composites containing sugarcane bagasse (25 wt%) and rice husk (0–10 wt%). They applied two types of pretreatment for the bagasse component, namely steaming and alkali treatment; however, the rice husk was pre-steamed in all cases. The authors found that the alkali treatment is more beneficial in regard to the flexural properties than the steaming. Pannu et al. [26] fabricated hybrid composites of PLA reinforced with banana waste and rice husk (up to 40 wt%) with 1:1 banana to rice husk ratios. It was found that both the flexural and tensile strength of PLA increased by around 2.5 times as a result of bio-reinforcement. Moreover, the impact strength reported was also roughly twice as compared to unfilled PLA.

In summary, there is an extensive literature available about biocomposites paired with specific biomass derivatives, however, there is much yet to be discovered regarding

the potentials in their hybridization considering the diversity of properties. The present research aims to utilize wood flour (WF) and RH waste simultaneously as potential fillers for PLA-based sustainable hybrid biocomposites. Throughout the experimental work, ternary composites with 0–10 wt% additives were prepared through extrusion followed by injection molding. The highest filler concentration was limited at 10 wt%, since above this level serious processability issues occurred due to the intensive degradation of the PLA matrix, which was also accompanied by drastically deteriorating toughness and strength, similar to what have already been reported in the literature for natural fiber reinforced biocomposites [27]. Subsequently, the influences of WF and RH on the mechanical, thermal, thermomechanical, and morphological properties of the PLA were investigated.

Materials and Methods

Materials

PLA pellets (Ingeo™ Biopolymer 2003D) were obtained from NatureWorks® LLC (Minnetonka, MN, USA). This PLA grade has a melting temperature of 170 °C, a density of 1.24 g/cm^3, and a number average molecular weight of ~ 100 500 g/mol.

Fine particles of North Indian rosewood (*Dalbergia sissoo*) WF were sourced from Krishna Timber store (Dadhol, Himachal Pradesh, India), while the RH was collected from a local farmer. The WF and RH particles that passed through a 60 mesh sieve (roughly 250 µm) were taken for composite preparation. Sieved particles were treated for 12 h with 2 wt% NaOH solution and oven-dried for 4 h at 80 °C after cleansing with distilled water. The SEM image of the WF and RH particles is presented in Fig. 1a, b, respectively.

Preparation and Processing

All the components were dried at 80 °C for 6 h in a DEGA-2500 type dehumidifier (DE.GA S.p.A., Corte Franca, Italy) before the melt compounding and prior to the injection molding procedure as well.

Biocomposites with a filler content of 0–10 wt% (WF:RH ratio 1:1) were prepared by means of melt mixing using an LTE 20–44 co-rotating twin-screw extruder (Labtech Engineering Co., Ltd., Samut Prakarn, Thailand) with an L/D ratio of 44 and a screw diameter of 20 mm. The screw speed was fixed at 30 rpm, while the temperature of the barrel (from feeder to die) was set to 155–185 °C. Subsequently, the extruded filaments were pelletized using a Labtech LZ120/VS type strand pelletizer (Labtech Engineering Co., Ltd., Samut Prakarn, Thailand). The composition and designation of the samples is collected in Table 1.

The prepared samples were injection molded into dumbbell-shaped specimens (EN ISO 527–2, type A) with an Allrounder Advance 420 C Golden Edition injection molding machine (Arburg, Lossburg, Germany). The injection unit's barrel temperature profile from feed zone to nozzle was the following: 175, 180, 185, 190, 195 °C. The screw diameter was 35 mm and the injection rate was set to 40 cm^3/s. The

Table 1 Composition and designation of the prepared samples

Designation	PLA content [wt%]	Rice husk content [wt%]	Wood flour content [wt%]
PLA	100	0	0
PLA_2.5	97.5	1.25	1.25
PLA_5	95	2.5	2.5
PLA_7.5	92.5	3.75	3.75
PLA_10	90	5	5

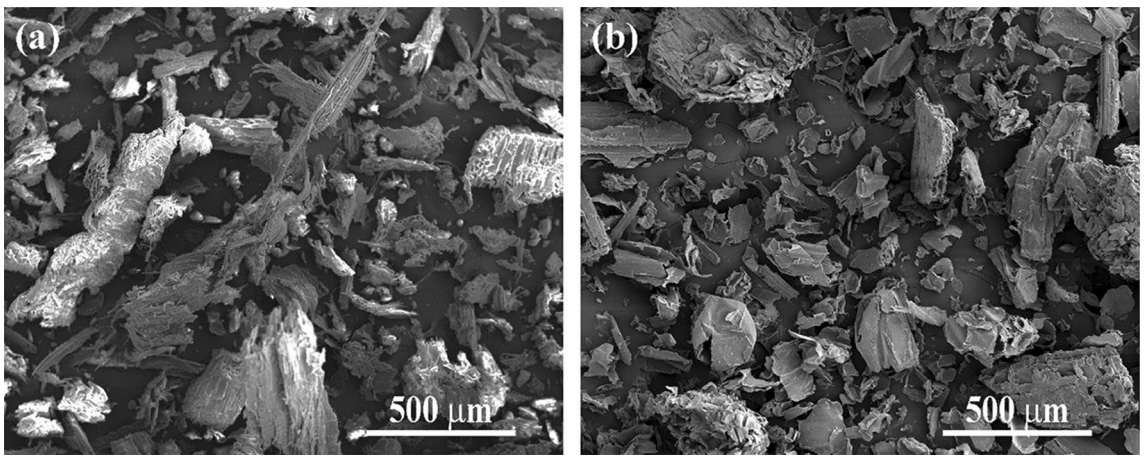

Fig. 1 The SEM image of the wood flour **a** and rice husk **b** particles

holding pressure profile was 750-650-250 bar (for a total of 15 s) and the mold temperature 35 °C.

Characterization

The surface morphology of PLA and its composites was studied using an S-3400 N (Hitachi, Tokyo, Japan) scanning electron microscope (SEM) with an acceleration voltage of 10 kV. The surfaces of the samples were sputter-coated using an SC7620 type sputter coater (Quorum Technologies Ltd, Laughton, UK) prior to the SEM inspection.

The quasi-static mechanical properties of the fabricated samples were tested on an Instron 5582 universal testing machine (Instron Ltd., Norwood, USA). The tensile strength, Young's modulus and elongation at break parameters were determined according to the EN ISO 527 standard at a crosshead travel speed of 5 mm/min (1 mm/min for Young's modulus). The flexural mechanical properties were measured according to the EN ISO 178 standard at a crosshead speed of 5 mm/min (1 mm/min when determining the flexural modulus). Flexural tests were carried out on rectangular specimens with a sample geometry of 80 × 4 × 10 mm (length, thickness and width, respectively) and a span length of 64 mm. Both measurements were repeated five times to obtain an average and a deviation.

Charpy impact tests were carried out in accordance with the standard EN ISO 179 using a Ceast 6545 impact testing machine (Ceast S.p.A., Pianezza, Italy). The impact energy was 2 J and the bearing distance was 62 mm. The specimens were un-notched, rectangular bars with a geometry of 80 mm × 4 mm × 10 mm. An average value of the Charpy impact strength and its standard deviation was calculated using five parallel measurements.

Differential scanning calorimetric measurements (DSC) were performed using a Netzsch DSC 200 F3 device (Netzsch-Gerätebau GmbH, Selb, Germany). The analyses were carried out with samples of ~5 mg weight in a nitrogen atmosphere. The following procedure was applied: heating from 30 to 200 °C at a rate of 5 °C/min then cooling down to 30 °C at the same rate. The whole process was performed twice; throughout the first one the thermal history of the samples were eliminated and throughout the second heating run the material properties were determined. The rate of crystallinity (X_c) was calculated based on Eq. (1) with an ideal melting enthalpy of PLA ($\Delta H_{\infty mPLA}$) taken as 93 J/g [28]:

$$x_c = \frac{\Delta H_{mPLA}}{\Delta H^{\infty}_{mPLA} \times \omega_{PLA}} \quad (1)$$

where ΔH_{mPLA} (J/g) is the melting enthalpy of PLA and ω_{PLA} is the weight fraction of PLA in the sample.

Dynamic mechanical analyses (DMA) were carried out in order to analyze the viscoelastic properties (i.e., storage modulus, loss factor) of the prepared samples. For this purpose a DMA Q800 machine (TA Instruments, New Castle, Delaware, USA) equipped with a dual cantilever grip was applied. A heating rate of 2 °C/min was used in the temperature range of 0–160 °C. The selected amplitude was 20 µm while the frequency was 1 Hz. The specimen was a rectangular bar with a length of 55 mm and a cross-section of 10 mm × 4 mm.

Analysis of variance (ANOVA) and the Tukey's honestly significant difference (HSD) test at a significance level of 5% ($p < 0.05$) were used to statistically evaluate the data obtained through the measurements.

Results and Discussion

Morphology Analysis

The fractured surfaces of PLA and the WF/RH-filled PLA composites obtained during the Charpy impact tests were studied using SEM to investigate the potential failure mechanism. The corresponding micrographs are presented in Fig. 2. Comparing the micrographs in Fig. 2, the pure PLA fractured surface (Fig. 2a) appeared to be smooth with no pores or voids and with some distinct river markings. Also, no signs of plastic deformation can be detected on the surface. Similar fracture characteristics have already been observed for unfilled PLA in the literature, and it was considered as an indication for its brittle characteristics [29]. The fractured surfaces of WF/RH filled PLA composites (Fig. 2b-e) showed a somewhat different behavior than pure PLA resin. The surroundings of the embedded fillers appeared to be smooth, similar to unfilled PLA indicating the brittle character of these composites. Similar results were reported in the literature for walnut shell filled PLA composites by Orue et al. [30]. In addition, some voids and gaps can also be observed between the interfacial region of PLA resin and the filler particles. The voids that are present between the components due to the improper adhesion between PLA and the particles are expected to generate concentrations of tensions during an impact load and result in a deterioration of impact mechanical properties as found experimentally. These facts are in agreement with the reduced strength values of the PLA composites with increased lignocellulosic fillers, well reported in the literature [24, 30, 31].

Tensile Mechanical Properties

The tensile mechanical properties of unfilled PLA and its WF and RH filled hybrid composites are collected in Table 2, while the typical tensile curves recorded during

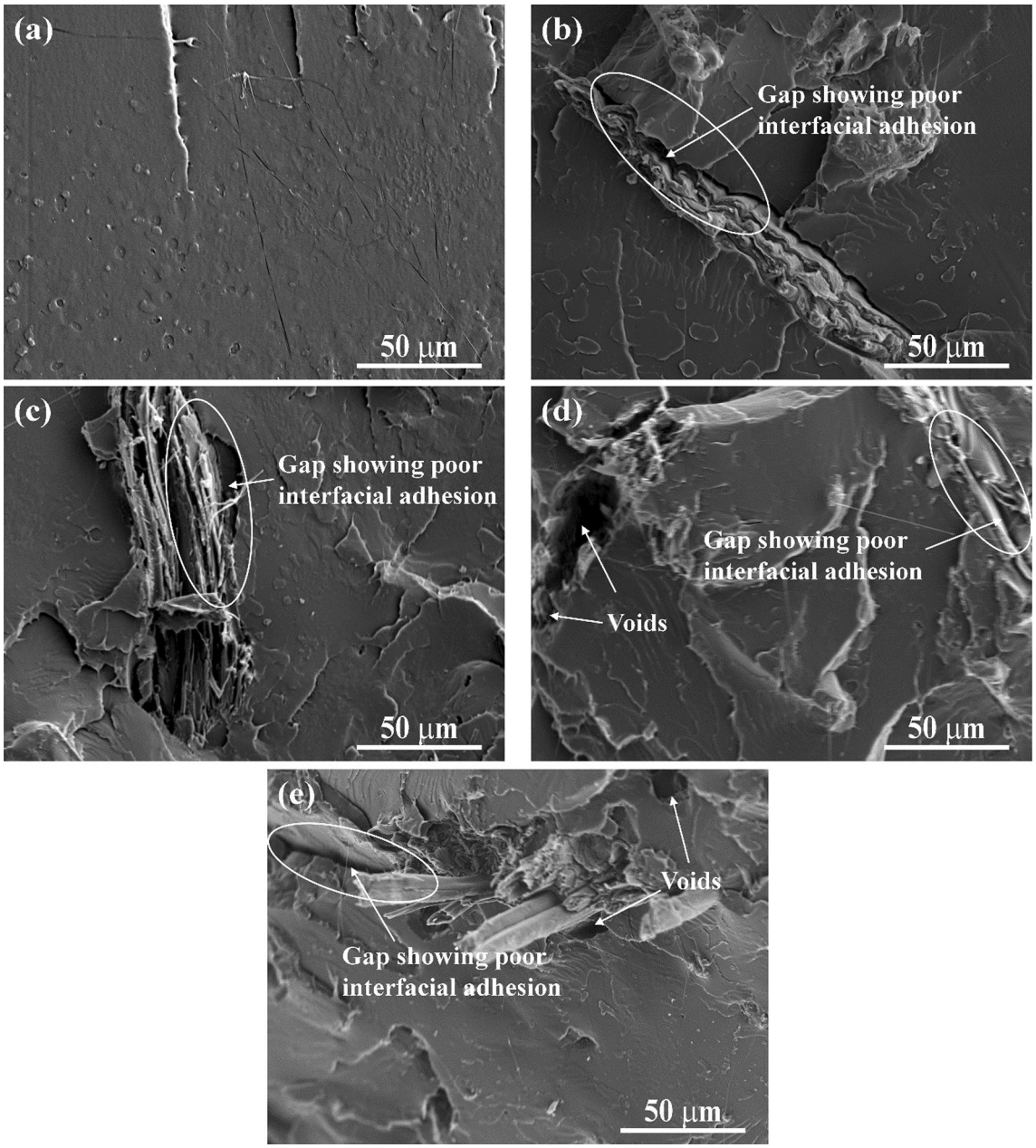

Fig. 2 Fracture surface morphology **a** PLA_0, **b** PLA_2.5, **c** PLA_5, **d** PLA_7.5 and **e** PLA_10

Table 2 Tensile mechanical properties of the PLA/WF/RH samples containing 0–10 wt% additives

Sample	Ultimate tensile strength [MPa]	Young's modulus [GPa]	Elongation at yield [%]	Elongation at break [%]
PLA	57.9 ± 0.3^{a}	2.56 ± 0.04^{a}	2.95 ± 0.15^{a}	5.22 ± 0.76^{a}
PLA_2.5	51.1 ± 1.0^{b}	2.77 ± 0.05^{b}	2.32 ± 0.03^{b}	2.70 ± 0.18^{b}
PLA_5	51.2 ± 1.4^{b}	$2.79 \pm 0.04^{b,c}$	$2.26 \pm 0.02^{b,c}$	2.58 ± 0.15^{b}
PLA_7.5	50.1 ± 0.3^{b}	2.89 ± 0.06^{c}	$2.15 \pm 0.03^{b,c}$	2.47 ± 0.14^{b}
PLA_10	50.2 ± 0.5^{b}	3.02 ± 0.05^{d}	2.11 ± 0.03^{c}	2.30 ± 0.17^{b}

Different letters in the superscripts (^{a,b,c,d}) indicate significant difference between the composites according to the Tukey's HSD test

the tensile tests for the various samples are presented in Fig. 3. It was clear that unfilled PLA exhibited superior ultimate tensile strength (57.9 MPa) but a lower Young's modulus (2.56 GPa), compared to any other compositions. The addition of 2.5 wt% WF/RH decreased the strength of PLA to 51.1 MPa, from this point; however, further addition of natural fillers did not result in any significant difference according to the statistical analyses. The strength values of 2.5–10 wt% WF/RH containing composites were all in the small range of 50.2–51.1 MPa, which is relatively lower than that of unfilled PLA by 11–13%. The reduced strength of the composites compared to unfilled PLA can be ascribed to the inadequate interfacial bonding between the matrix material and the additives. Similar results, namely poor adhesion and limited strength, were reported in the literature for various combinations of hydrophobic polymer / hydrophilic natural fiber composites[32, 33]. On the other hand, a gradual improvement in Young's modulus was observed with increasing filler content, peaking at 3.02 GPa for the PLA_10 sample, which is a relative increment of 18%, compared with PLA. The superior modulus of the composites is attributed to the higher stiffness of the incorporated fibers compared to the matrix material. The elongation at yield and the elongation at break of PLA gradually declined as a function of WF/RH concentration, bottoming at 2.11% and 2.30%, respectively.

Comparing these results to our previous experiments [34, 35], where only WF was used as filler without the addition of RH, it can be concluded that the presence of the latter additive results in a slightly lower strength (50.2 MPa vs. 50.9 MPa – at 10 wt% overall filler content) and deformability (2.3% vs. 2.4% – elongation at break at 10 wt% overall filler content), and a higher modulus (3.02 GPa vs. 2.97 GPa – at 10 wt% overall filler content). This can be ascribed to a more rigid characteristics of rice waste compared to wood particles. Besides, those literatures dealing with the preparation of RH-filled PLA composites mostly report intensive reduction in tensile strength paired with excellent modulus due to the rigid nature of this filler particle [36, 37].

Table 3 Flexural mechanical properties of the PLA/WF/RH samples containing 0–10 wt% additives

Sample	Flexural stress at conventional deflection [MPa]	Flexural modulus [GPa]
PLA	99.5 ± 0.2^{a}	3.43 ± 0.02^{a}
PLA_2.5	99.7 ± 0.6^{a}	3.58 ± 0.02^{b}
PLA_5	99.3 ± 0.9^{a}	3.69 ± 0.07^{c}
PLA_7.5	$97.8 \pm 0.5^{a,b}$	3.92 ± 0.03^{d}
PLA_10	$97.4 \pm 1.4^{b,*}$	4.03 ± 0.03^{e}

Different letters in the superscripts (^{a,b,c,d,e}) indicate significant difference between the composites according to Tukey's HSD test

An asterisk in the superscript (*) means that flexural strength values instead of flexural stress at conventional deflection are given, as the specimens broke before reaching the point of conventional deflection

Flexural Mechanical Properties

The flexural properties of unfilled PLA and its WF and RH filled hybrid composites are collected in Table 3, while the typical flexural curves recorded during the 3-point bending tests for the various samples are presented in Fig. 4. Following the ISO 178 standard, for specimens (PLA, PLA_2.5, PLA_5, PLA_7.5) that did not break until the point of conventional deflection the flexural stress at conventional deflection values were reported, while for the sample that broke earlier than this point (PLA_10) the flexural strength was given. Based on the results summarized in Table 3, it

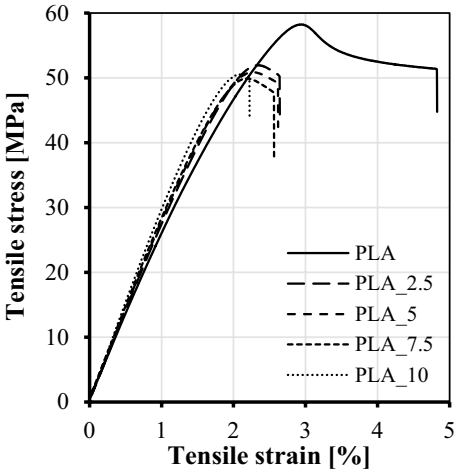

Fig. 3 Typical tensile curves of the PLA/WF/RH composites containing 0–10 wt% additives

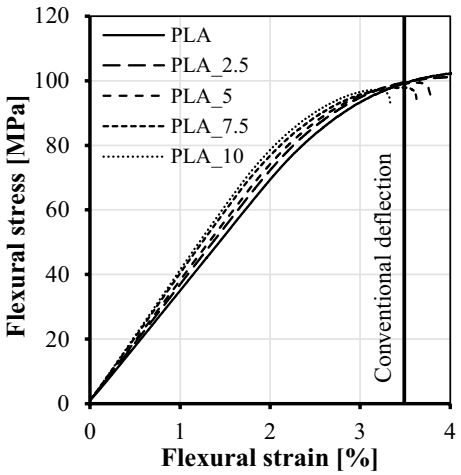

Fig. 4 Typical flexural curves of the PLA/WF/RH composites containing 0–10 wt% additives

can be concluded that the calculated strength of the different PLA composites was in a relatively small range of 97.4–99.7 MPa, peaking at 2.5 wt% WF/RH content. It has to be noted that according to the statistical analysis there wasn't any significant difference in the strength of the samples, except the PLA_10 composite, which exhibited a slightly lower strength compared to the other ones.

Contrary to the strength, the flexural modulus of the composites was found to gradually rise with increasing filler content. The lowest modulus (3.43 GPa) was exhibited by the neat PLA, which then increased to 3.58 GPa. 3.69 GPa, 3.92 GPa and 4.03 GPa at 2.5 wt%, 5 wt%, 7.5 wt% and 10 wt% of WF/RH loading, respectively. Again, the increased modulus can be attributed to the high stiffness of filler particles. The reason that the fillers to are able increase the stiffness of PLA without providing superior strength can be explained by the poor interfacial bonding between the components as it was shown in the SEM images previously (Fig. 2). While an improvement in strength could only be achieved with proper adhesion, interfacial bonding does not play a crucial role when it comes to the stiffness of multicomponent materials.

Overall, similar to the tensile test results, higher modulus was found when using WF and RH hybrid filling, compared to those samples containing solely the WF [34]; however, at a cost of slightly lower strength, which can be ascribed to the more rigid characteristics of rice waste compared to wood. Yussuf et al. [38] also concluded in their study dealing with the characterization of natural fiber reinforced PLA-based composites that the incorporation of RH tends to reduce the flexural strength of the PLA matrix. Dimzoski et al. [36] achieved similar results as well for PLA/RH composites, reporting a drastic drop (-43.3%) in the flexural stress above 20 wt% filler content.

Impact Strength

Impact strength is defined as the ability of the material to withstand fracture under stress applied at high speed. The effect of WF/RH content on the Charpy impact strength of the prepared samples is depicted in Fig. 5. Considering the impact strength, neat PLA (15.3 kJ/m^2) outperformed all the other composites investigated in this experimental study. Even a 2.5 wt% WF/RH addition caused a relative decrement of 25% in the toughness of PLA. However, for composites with further filler content there was no significant change found, the impact strength of all PLA/WF/RH materials was in the range of 8.8–11.4 kJ/m^2. Organic fillers, such as rice waste and wood waste, tend to be highly stiff, as already concluded throughout the discussion of tensile and flexural tests. High stiffness in most cases is accompanied with considerable rigidity too. The incorporation of these rigid fillers is assumed to be one of the foremost reasons for the drop in toughness. On the other hand, the voids that

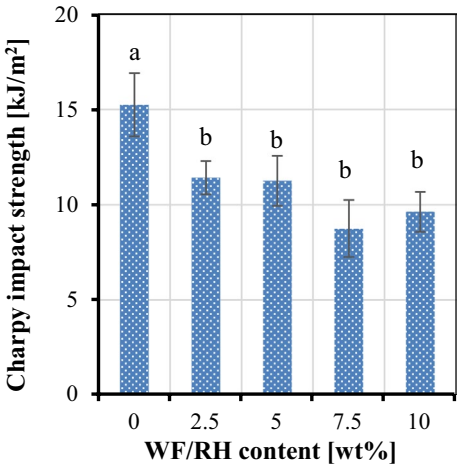

Fig. 5 Charpy impact strength of PLA/WF/RH samples containing 0–10 wt% additives. The different letters (a, b) above the columns indicate significant difference among composites according to Tukey's HSD test ($p < 0.05$)

are present between the components due to the improper adhesion between PLA and the particles (also observed on the SEM images) generate concentrations of tensions during an impact load, and this results in a deterioration of impact mechanical properties as well. Comparing the results of PLA/WF/RH ternary composites with PLA-based composites filled only with wood waste [34] it can be concluded that the introduction of RH slightly decreased the impact resistance of the biocomposites. This is in good accord with the improved modulus values of RH containing composites determined throughout the tensile and flexural tests, since higher stiffness generally comes with a more rigid behavior. Similar results, namely reduced impact resistance was reported in the literature for rice husk-filled composites of various polymer matrices, including PLA [37–39].

DSC Results

The results obtained during the second heating run of differential scanning calorimetry for PLA and its WF/RH-filled composites are collected in Table 4, while the corresponding DSC curves are presented in Fig. 6. The first thermal transition exhibited by the unfilled PLA during the measurement was the glass transition at 58.7 °C. The T_g was followed by cold crystallization (T_{cc}), marked by an exothermic peak. The presence of cold crystallization indicates that chain molecules could not arrange during cooling down due to the slow crystallization kinetics of polymer molecules; therefore, the PLA matrix after cooling was rather amorphous. Apparently, in the temperature range of 90–125 °C the increased chain mobility facilitated the arrangement of PLA molecules. With further increase in temperature, a double endothermic peak occurred in

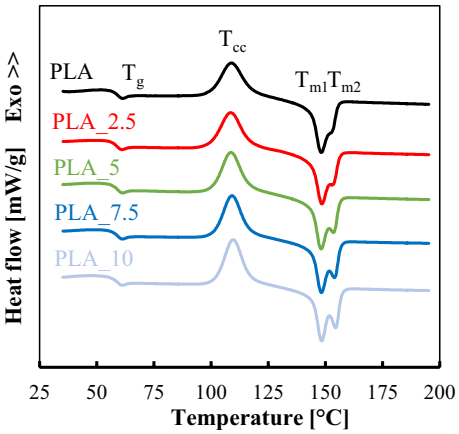

Fig. 6 Characteristic DSC curves of PLA/WF/SH samples registered during thesecond heating run

the range of 125–160 °C corresponding to the melting of the semi-crystalline structure. Out of the two endothermic peaks, the first one, T_{m1} (148.2 °C), was considered to be the major, while the second one, T_{m2} (152.5 °C), was barely noticeable for unfilled PLA. For the double melting peak, multiple hypotheses have been introduced in the literature [40, 41]. According to Yasuniwa et al. [40], parallel to the melting of PLA, a melt-recrystallization process is also taking place, resulting in the less perfect crystallites being transformed successively into more stable ones. This model suggests that there are two crystalline species present in PLA, out of which one is less ordered, than the other. Since the recrystallization is a time-consuming process, the quantity of the recrystallized crystals is limited and it is dependent on multiple factors. For instance, the inclusion of reinforcement particles tend to promote the formation of the more organized PLA crystals [42]. The other hypothesis explains the double melting peak by two versions of the same crystallite being present, one of which is less stable (α'), thereby exhibiting a lower melting temperature than the stable type (α). According to this theory, the ratio of the α and α' crystallites depends on the temperature where they were formed. When crystallization takes place below 120 °C, then α' is the preferred type, while above this temperature it is α. The enthalpy measured during cold crystallization and the melting was rather similar, 24.1 J/g and 24.2 J/g, respectively, which confirms that little to no crystallites were formed during the cooling run. The rate of crystallinity determined for PLA based on Eq. (1) is 26%; however, it needs to be noted that it can only be applied for the small temperature range around ~125 °C where the cold crystallization already finished and before the polymer started to melt. Other than that, the PLA was rather amorphous.

The DSC curves of PLA/WF/RH composites were quite similar to that of unfilled PLA with some obvious differences. The T_g of all samples was found in the small range of 59 ± 0.3 °C, no discernible pattern based on the filler content was observed. On the other hand, there was an obvious trend in the cold crystallization temperature values that slightly increased gradually from 108.7 °C to 109.7 °C with growing filler loading. Parallel to this, the ratio of the two melting peaks also shifted, the second one became more and more dominant. Depending on which theory of double melting is applied, it can either mean that (i) the presence of WF/RH particles promoted the recrystallization phenomenon by increasing the quantity of the recrystallized crystals, or that (ii) the slightly increased T_{cc} led to the formation of more stable α crystalline types compared to the less stable α'. In order to more thoroughly understand the alterations of crystalline variants, further X-Ray diffraction analysis would be required to perform in the future. The melting enthalpy (ΔH_m) of the samples also increased with the growing amount of WF/RH filler, which refers to a change in crystallinity. In fact, the initial degree of crystallinity (X_c) of PLA (26.0%) increased by 6.3% when 10 wt% of WF/RH was incorporated into the polymer, which means that these natural additives facilitated the crystallization of PLA. Similar results have already been reported in the literature for PLA-based composites filled various natural fillers [8, 43, 44]. Since the growth in crystallinity was much more prominent than what was previously found for PLA-composites filled only with WF (1.7%) [34], it can be concluded that RH is a more efficient nucleating agent in the hybrid system.

Table 4. DSC data of the PLA/WF/RH obtained from the second heating curves.

Sample	T_g [°C]	T_{cc} [°C]	ΔH_{cc} [J/g]	T_{m1} [°C]	T_{m2} [°C]	ΔH_m [J/g]	X_c [%]
PLA	58.7	108.7	24.1	148.2	152.5	24.2	26.0
PLA_2.5	59.3	108.8	24.8	148.2	152.9	25.0	27.6
PLA_5	59.0	108.8	25.5	148.2	153.5	25.7	29.1
PLA_7.5	59.1	109.0	25.6	148.3	153.9	25.8	30.0
PLA_10	58.9	109.7	25.7	148.3	154.4	27.0	32.3

T_g glass transition temperature, T_{cc} cold crystallization temperature, ΔH_{cc} enthalpy of cold crystallization, T_m melting temperature, ΔH_m enthalpy of melting, X_c degree of crystallinity of PLA

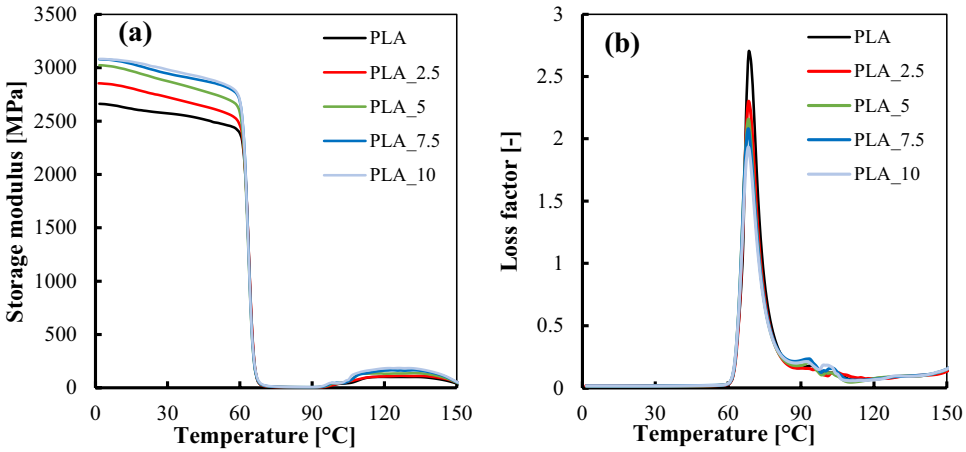

Fig. 7 Storage modulus (**a**) and loss factor (**b**) as a function of temperature for PLA and its WF/RH-filled biocomposites

DMA Analysis

The storage modulus (*E'*) and the loss factor (*tan δ*) values of PLA and its WF/RH-filled composites as a function of temperature are shown in Fig. 7. According to Fig. 7a the storage modulus of PLA shows a gradually declining trend up until 60 °C, after which a sudden drop can be observed in the range of 60–66 °C, corresponding to the glass transition temperature (T_g) of the polymer. The reason for the T_g being slightly higher in this case than the one measured with the DSC technique is that DMA is performed at a specific frequency and thus the observed transition is the dynamic glass-to-rubber transition process, whereas through DSC the calorimetric glass-to-rubber transition temperature was determined. As a consequence of exceeding the T_g temperature, the PLA exhibited its first rubbery plateau where the storage modulus bottomed at 5 MPa. Due to polymer chains having sufficient mobility in this state, development of crystalline regions occurred, leading to the regaining of part of the lost storage modulus in the temperature range of 95–110 °C [45]. The cold crystallization was followed by the second rubbery plateau from 110 to 140 °C. In this zone the *E'* of PLA increased up to 100 MPa, which can be attributed to the confinement effect of newly formed crystalline regions on the amorphous phases [46]. Above 140 °C the storage modulus declined once more due to the beginning of the melting. Regarding the loss factor (*tan δ*), a single major peak was observed for neat PLA. The presence of such sharp, intense peaks is typical for unfilled polymers since there is no additive that would hinder the polymer chain mobility [47].

In the case of WF/RH-filled composites, the characteristics of the DMA curves appeared to be quite similar to neat PLA with some differences. Firstly, the storage modulus of the fabricated samples obviously increased with growing filler content throughout the whole measurement. Meanwhile, the T_g of the composites did not shift either to lower or to higher temperatures, which is in good agreement with DSC results and this can be attributed to the limited interactions between the PLA matrix and natural particles used as additives. Upon incorporation of WF/RH, there is a gradual reduction in *tan δ* peak height, which can be explained by the restriction of chain mobility caused by the presence of filler particles.

Conclusion

In this study, the applicability of wood waste and rice husk was investigated as fillers for biopolymer-based composites. Composite samples were prepared using a twin-screw extruder and formed into specimens suitable for characterization as per injection molding. SEM images revealed a brittle fracture, which is typical for PLA. Meanwhile, in the WF/RH-filled composites voids were observed due to the improper adhesion between PLA and the natural particles. Gradually improving modulus values were found both during the tensile and 3-point bending tests with growing WF/RH content. Both the tensile strength and impact strength exhibited a slight drop when the lowest amount of fillers (2.5 wt%) was incorporated; however, no significant decrease occurred in either of these properties for further particle loading. The values of flexural stress at conventional strain showed little to no change up until the highest (10 wt%) filler concentration, and even at that point only a slight decrease of 2 MPa was detected. The thermal analyses showed that the glass transition temperature of PLA was not affected by additives. On the other hand, according to the DSC traces, the cold crystallization temperature of PLA shifted to a slightly higher temperature, which also affected the crystalline structure of the fabricated biocomposites. Meanwhile, the incorporated particles acted as nucleating agents, leading to a higher crystalline ratio.

It can be concluded that amalgamation of wood waste and rice husk in PLA-based composites can be considered advantageous, since all evaluated properties either improved or only slightly dropped, while a substantial amount of PLA was replaced by waste materials that are essentially free. Considering these facts, the found benefits and decreased overall production cost are expected to promote PLA as an eco-friendly material worldwide.

Acknowledgements L. Lendvai is grateful for the support of the János Bolyai Research Scholarship of the Hungarian Academy of Sciences. L. Lendvai is also grateful for the National Scholarship Programme of the Slovak Republic.

Author Contributions Each author participated sufficiently in the work. LL, TS and GD produced the samples and conducted the mechanical tests. LL, AP and MO performed the morphological, thermal and thermomechanical analyses. LL and TS wrote the main manuscript text. All authors reviewed the manuscript.

Funding Open access funding provided by Széchenyi István University (SZE). The work reported here was supported by the National Talent Programme – Hungary through the project NTP-NFTÖ-21-B. This work was partially supported through the project VEGA 02/0006/22 (Slovakia).

Declarations

Conflict of interest The authors have no competing interests as defined by Springer, or other interests that might be perceived to influence the results and/or discussion reported in this paper.

References

1. Jost V (2018) Packaging related properties of commercially available biopolymers – an overview of the status quo. Express Polym Lett 12:429–435
2. Nakagaito AN, Fujimura A, Sakai T, Hama Y, Yano H (2009) Production of microfibrillated cellulose (MFC)-reinforced polylactic acid (PLA) nanocomposites from sheets obtained by a papermaking-like process. Compos Sci Technol 69:1293–1297
3. Bouzouita A, Notta-Cuvier D, Raquez JM, Lauro F, Dubois P (2018). In: DiLorenzo ML, Androsch R (eds) Industrial applications of poly(Lactic Acid). Springer International Publishing Ag, Cham
4. Wang L, Tong Z, Ingram LO, Cheng Q, Matthews S (2013) Green composites of poly (Lactic Acid) and sugarcane bagasse residues from bio-refinery processes. J Polym Environ 21:780–788
5. Lendvai L, Brenn D (2020) Mechanical, morphological and thermal characterization of compatibilized poly(Lactic Acid)/thermoplastic starch blends. ActaTechJaur 13:1–13
6. Muller J, Gonzalez-Martinez C, Chiralt A (2017) Combination of poly(lactic) acid and starch for biodegradable food packaging. Materials 10:952
7. Fekete I, Ronkay F, Lendvai L (2021) Highly toughened blends of poly(lactic acid) (PLA) and natural rubber (NR) for FDM–based 3D printing applications: the effect of composition and infill pattern. Polym Test 99:107205
8. Battegazzore D, Noori A, Frache A (2019) Natural wastes as particle filler for poly(lactic acid)-based composites. J Compos Mater 53:783–797
9. Lendvai L, Singh T, Fekete G, Patnaik A, Dogossy G (2021) Utilization of waste marble dust in poly(Lactic Acid)-based biocomposites: mechanical, thermal and wear properties. J Polym Environ 29:2952–2963
10. Zheng H, Sun Z, Zhang H (2019) Effects of walnut shell powders on the morphology and the thermal and mechanical properties of poly(lactic acid). J Thermoplast Compos Mater 33:1383–1395
11. Petrény R, Tóth C, Horváth A, Mészáros L (2022) Development of electrically conductive hybrid composites with a poly(lactic acid) matrix, with enhanced toughness for injection molding, and material extrusion-based additive manufacturing. Heliyon 8:e10287
12. Shang H, Ke L, Xu W, Shen M, Fan Z-X, Zhang S, Wang Y, Tang D, Huang D, Yang H-R, Zhou D, Xu H (2022) Microwave-assisted direct growth of carbon nanotubes at graphene oxide nanosheets to promote the stereocomplexation and performances of polylactides. Ind Eng Chem Res 61:1111–1121
13. Väisänen T, Haapala A, Lappalainen R, Tomppo L (2016) Utilization of agricultural and forest industry waste and residues in natural fiber-polymer composites: a review. Waste Manag 54:62–73
14. Chandrasekhar S, Satyanarayana KG, Pramada PN, Raghavan P, Gupta TN (2003) Review processing, properties and applications of reactive silica from rice husk—an overview. J Mater Sci 38:3159–3168
15. Ezenkwa OE, Hassan A, Samsudin SA (2021) Influence of different surface treatment techniques on properties of rice husk incorporated polymer composites. Rev Chem Eng 37:907–930
16. Raghu N, Kale A, Chauhan S, Aggarwal PK (2018) Rice husk reinforced polypropylene composites: mechanical, morphological and thermal properties. J Indian Acad Wood Sci 15:96–104
17. Lim SL, Wu TY, Sim EYS, Lim PN, Clarke C (2012) Biotransformation of rice husk into organic fertilizer through vermicomposting. Ecol Eng 41:60–64
18. Ezenkwa OE, Hassan A, Samsudin SA (2022) Mechanical properties of rice husk and rice husk ash filled maleated polymers compatibilized polypropylene composites. J Appl Polym Sci 139:51702
19. de Matos Costa AR, Lima JC, dos Santos R, Barreto LS, Henrique MA, de Carvalho LH, de Almeida YMB (2021) Rheological, thermal and morphological properties of polyethylene terephthalate/polyamide 6/rice husk ash composites. J Appl Polym Sci 138:50916
20. Sirichalarmkul A, Kaewpirom S (2021) Enhanced biodegradation and processability of biodegradable package from poly(lactic acid)/poly(butylene succinate)/rice-husk green composites. J Appl Polym Sci 138:50652
21. Mu B, Tang W, Liu T, Hao X, Wang Q, Ou R (2021) Comparative study of high-density polyethylene-based biocomposites reinforced with various agricultural residue fibers. Ind Crops Prod 172:114053
22. Farhan Zafar M, Siddiqui MA (2018) Raw natural fiber reinforced polystyrene composites: effect of fiber size and loading. Mater Today:Proc 5:5908–5917

23. Borysiuk P, Boruszewski P, Auriga R, Danecki L, Auriga A, Rybak K, Nowacka M (2021) Influence of a bark-filler on the properties of PLA biocomposites. J Mater Sci 56:9196–9208
24. Andrzejewski J, Szostak M, Barczewski M, Łuczak P (2019) Cork-wood hybrid filler system for polypropylene and poly(lactic acid) based injection molded composites. Structure evaluation and mechanical performance. Compos Part B: Eng 163:655–668
25. Anggono J, Budiarto B, Sugondo S, Purwaningsih H (2020) Antoni, the strength of polylactic acid composites reinforced with sugarcane bagasse and rice husk. Mater Sci Forum 1000:193–199
26. Pannu AS, Singh S, Dhawan V, Singh JIP (2021) Sustainable use of agri-waste in the production of green hybrid composites. Sustainable development through engineering innovations. Springer, Singapore, pp 125–132
27. Berthet MA, Angellier-Coussy H, Chea V, Guillard V, Gastaldi E, Gontard N (2015) Sustainable food packaging: Valorising wheat straw fibres for tuning PHBV-based composites properties. Compos Part A: Appl Sci Manufac 72:139–147
28. Battegazzore D, Bocchini S, Frache A (2011) Crystallization kinetics of poly(lactic acid)-talc composites. Express Polym Lett 5:849–858
29. Xu H, Zhou J, Odelius K, Guo Z, Guan X, Hakkarainen M (2021) Nanostructured phase morphology of a biobased copolymer for tough and UV-resistant polylactide. ACS Appl Polym Mater 3:1973–1982
30. Orue A, Eceiza A, Arbelaiz A (2020) The use of alkali treated walnut shells as filler in plasticized poly(lactic acid) matrix composites. Ind Crops Prod 145:111993
31. Silva CG, Campini PAL, Rocha DB, Rosa DS (2019) The influence of treated eucalyptus microfibers on the properties of PLA biocomposites. Compos Sci Technol 179:54–62
32. Robledo-Ortíz JR, Martín del Campo AS, Blackaller JA, González-López ME (2021) Pérez Fonseca, valorization of sugarcane straw for the development of sustainable biopolymer-based composites. Polym (Basel) 13:3335
33. Kuciel S, Mazur K, Hebda M (2020) The influence of wood and basalt fibres on mechanical, thermal and hydrothermal properties of PLA composites. J Polym Environ 28:1204–1215
34. Singh T, Lendvai L, Dogossy G, Fekete G (2021) Physical, mechanical, and thermal properties of Dalbergia sissoo wood waste-filled poly(lactic acid) composites. Polym Compos 42:4380–4389
35. Singh T, Patnaik A, Ranakoti L, Dogossy G, Lendvai L (2022) Thermal and Sliding wear properties of wood waste-filled poly(Lactic Acid) biocomposites. Ploymers (Basel) 14:2230
36. Dimzoski B, Bogoeva-Gaceva G, Gentile G, Avella M, Errico ME, Srebrenkoska V (2008) Preparation and characterization of poly(lactic acid)/rice hulls based biodegradable composites. J Polym Eng 28:369–384
37. Arjmandi R, Hassan A, Majeed K, Zakaria Z (2015) Rice husk filled polymer composites. Int J Polym Sci 2015:501471
38. Yussuf AA, Massoumi I, Hassan A (2010) Comparison of polylactic acid/kenaf and polylactic acid/rise husk composites: the influence of the natural fibers on the mechanical, thermal and biodegradability properties. J Polym Environ 18:422–429
39. Mohammadi-Rovshandeh J, Pouresmaeel-Selakjani P, Davachi SM, Kaffashi B, Hassani A, Bahmeyi A (2014) Effect of lignin removal on mechanical, thermal, and morphological properties of polylactide/starch/rice husk blend used in food packaging. J Appl Polym Sci 131:41095
40. Yasuniwa M, Tsubakihara S, Sugimoto Y, Nakafuku C (2004) Thermal analysis of the double-melting behavior of poly(L-lactic acid). J Polym Sci Part B: Polym Phys 42:25–32
41. Ambrosio-Martín J, Fabra MJ, Lopez-Rubio A, Lagaron JM (2014) An effect of lactic acid oligomers on the barrier properties of polylactide. J Mater Sci 49:2975–2986
42. Xu H, Ke L, Tang M, Shang H, Zhang Z-L, Xu W, Fu Y-N, Wang Y, Tang D, Huang D, Zhang S, Yang H-R, He X, Gao J (2022) Pea pod-mimicking hydroxyapatite nanowhisker-reinforced poly(lactic acid) composites with bone-like strength. Int J Biol Macromol 216:114–123
43. Xu H, Xie L, Chen Y-H, Huang H-D, Xu J-Z, Zhong G-J, Hsiao BS, Li Z-M (2013) Strong shear flow-driven simultaneous formation of classic shish-kebab, hybrid shish-kebab, and transcrystallinity in poly(Lactic Acid)/natural fiber biocomposites. ACS Sustain Chem Eng 1:1619–1629
44. Masirek R, Kulinski Z, Chionna D, Piorkowska E, Pracella M (2007) Composites of poly(L-lactide) with hemp fibers: morphology and thermal and mechanical properties. J Appl Polym Sci 105:255–268
45. Mofokeng JP, Luyt AS, Tábi T, Kovács J (2012) Comparison of injection moulded, natural fibre-reinforced composites with PP and PLA as matrices. J Thermoplast Compos Mater 25:927–948
46. Cristea M, Ionita D, Iftime MM (2020) Dynamic mechanical analysis investigations of pla-based renewable materials: how are they useful? Materials 13:5302
47. Petinakis E, Yu L, Edward G, Dean K, Liu H, Scully AD (2009) Effect of matrix–particle interfacial adhesion on the mechanical properties of poly(Lactic Acid)/wood-flour micro-composites. J Polym Environ 17:83